PHYSICAL REVIEW D **76,** 061502(R) (2007)

Binary black hole mergers: Large kicks for generic spin orientations

Wolfgang Tichy and Pedro Marronetti

Department of Physics, Florida Atlantic University, Boca Raton, Florida 33431, USA

(Received 14 March 2007; revised manuscript received 25 May 2007; published 10 September 2007)

We present results from several simulations of equal mass black holes with spin. The spin magnitudes are $S/m^2 = 0.8$ in all cases, but we vary the spin orientations arbitrarily, inside and outside the orbital plane. We find that in all but one case the final merged black hole acquires a kick of more than 1000 km/s, indicating that kicks of this magnitude are likely to be generic and should be expected for mergers with general spin orientations. The maximum kick velocity we find is 2500 km/s and occurs for initial spins which are antialigned in the initial orbital plane.

DOI: 10.1103/PhysRevD.76.061502 PACS numbers: 04.25.Dm, 04.30.Db, 04.70.Bw, 97.60.Lf

I. INTRODUCTION

Currently several laser-interferometric gravitational wave detectors such as TAMA [1], LIGO [2], and GEO [3] are already operating, while several others are in the planning or construction phase [4]. One of the most promising sources for these detectors are the inspirals and mergers of binary black holes. The gravitational waves radiated during the inspiral and merger of two black holes carry energy, linear momentum, and angular momentum fluxes. The radiated energy is positive and thus the system will always lose energy. Except in the case of certain highly symmetric situations, such as head-on collisions of equal mass nonspinning black holes, the system usually also loses angular momentum. Generic systems with either unequal masses or spins with no particular alignment will also radiate linear momentum, resulting in a nonzero residual velocity (also known as recoil or ''kick'') of the final black hole. The magnitude of this recoil is important in a variety of astrophysical scenarios, such as the cosmological evolution of supermassive black holes [5–12] or the growth and retention of intermediate-mass black holes in dense stellar clusters [13–19]. For a binary in almost circular orbit, the direction of the instantaneous linear momentum flux rotates in the orbital plane with the angular velocity of the system. Thus, when the binary goes through one orbital period, the average linear momentum flux will be close to zero. The only net effect comes from the fact that the inspiral orbits are not perfect circles. Most of the kick is thus accumulated during the last orbit and subsequent plunge of the two holes, when the motion of the two holes is no longer quasicircular and the averaged linear momentum flux is much larger. Several analytical estimates of the kick velocity have been published in recent years [20–23]. All these estimates have been derived using approximations (such as post-Newtonian theory) which break down during the last orbit and the subsequent merger. Hence these calculations contain a high degree of uncertainty. In addition, there are calculations which employ the close limit approximation [24,25]. However, these calculations can only model the plunge well, and miss contributions from the last orbit. There is also an analytic calculation based on attaching quasinormal ringdown modes to post-Newtonian waveforms [26]. Furthermore, results from several numerical simulations have been published [27–35] recently. The resulting maximum kick velocities found so far are 175 km/s for nonspinning unequal mass black holes [29], 257 km/s for equal mass black holes with unequal spins aligned with the orbital angular momentum [31], and 2500 km/s for equal mass black holes with antialigned spins $S/m^2 \approx \pm 0.8$ in the orbital plane [33]. The latter value is so high that the final black hole would escape e.g. both from dwarf elliptical and spheroidal galaxies (with typical escape velocities of below 300 km/s) and from giant elliptical galaxies (2000 km/s) [5]. Extrapolations from simulations of black hole binaries with spins in the orbital plane predict velocities as high as 4000 km/s [34]. The question thus arises if such high kick velocities are generic for spinning black holes, or if the results of 2500 km/s or even 4000 km/s arise only if the initial spins are exactly antialigned and confined to the initial orbital plane. To answer this question we have performed several simulations of black hole binaries on initially approximately circular orbits with spins in arbitrary directions. We find that except for one case the kick velocities are well above 1000 km/s. Thus, kicks of this magnitude seem to be a generic feature of black hole mergers with spin around or above $S/m^2 \approx 0.8$.

II. NUMERICAL TECHNIQUES

Our simulations are performed using the ''moving punctures'' method [36,37] with the BAM code [38,39] which allows us to use moving nested refinement boxes. We use 10 levels of 2:1 refinements. The outer boundaries are located $240M$ away from the initial center of mass (M being the sum of the initial black hole masses), and our resolution ranges between $9M$ on the outermost box to $M/56.9$ near the black holes. Since our simulations have no particular symmetries, we cannot use the usual memory saving techniques and simulate only one quadrant of the numerical domain. Thus, our simulations take 4 times more memory and time than e.g. the ones reported in

[40]. This makes standard convergence tests very costly. Thus, the goal of this work is merely to give kick velocity estimates which can be used in astrophysics, instead of extremely accurate results. For the same reason, we present a convergence test for only one particular case in order to establish that our numerical setup gives results that are in the convergent regime. In Fig. 1 we show the energy radiated during the merger of a binary where both initial spins have magnitude $S/m^2 = 0.8$ and are antialigned to the orbital angular momentum. From the upper panel we see that the results for the three resolutions are consistent and very close to each other. The lower panel shows the difference between the low and medium, and also between the medium and high resolutions. The latter difference has been scaled such that the two curves would coincide for exact fourth order convergence. This order of convergence, however, is only approximately achieved, even though our code employs a fourth order accurate finite differencing scheme. Nonetheless, we take this result to mean that the resolutions h_1, h_2, and h_3 are sufficiently close to the convergent regime to give at least qualitatively reliable results. All other results, which are given below, have been obtained using the lowest resolution $h_1 = M/56.9$. Assuming approximately fourth order convergence it would be possible to obtain error bars due to the finite differencing scheme used here. These error bars would be on the order of a few percent. Notice, however, that there are other sources of errors, the biggest of which is the extraction of the radiated energy and momentum at a finite radius. This radius should ideally be far from the sources. However, the outer regions of our grid are not very well resolved, since the highly refined boxes do not extend far from each black hole. We find that the best compromise for our grid structure is to extract at $r_{\rm ex} \sim 30M$. Figure 2 shows the radiated momentum in the z direction extracted at different radii. In this example both initial spins are perpendicular to each other and lie in the initial orbital plane. The first three curves (thick lines) at $r_{\rm ex} = 20M$, $30M$, and $40M$ come from a run with our standard grid setup. In this case the grid resolutions at these radii are $h_{\rm ex} = 1.125M$ at the two inner radii but only $h_{\rm ex} = 2.25M$ at $r_{\rm ex} = 40M$. This explains why the difference between the $30M$ and $40M$ results is not smaller than between the $30M$ and $20M$ results. We have also performed a second run (thin lines) where we have enlarged some of our refinement boxes. In this run $r_{\rm ex} = 40M$ is now located on a level with $h_{\rm ex} = 1.125M$ as well. If we compare the results $r_{\rm ex} = 20M$, $30M$, and $40M$ for $h_{\rm ex} = 1.125M$, we see that the difference between the $30M$ and $40M$ results is now smaller than the difference between the $30M$ and $20M$ results, as expected. In the run with the enlarged refinement boxes, the result for $r_{\rm ex} = 30M$ remains unchanged (at the level of accuracy of this plot) because the resolution at $r_{\rm ex} = 30M$ is unchanged, while there is a small difference for the $r_{\rm ex} = 20M$ result (thin dashed line), because this radius is now located on an even better resolved level. The differences between these results at different radii and resolutions provide an estimate of the error due to extraction at a finite extraction radius. As a conservative estimate we use the average relative difference between the $30M$ and $40M$ results (at $t = 300M$) over all our simulations with the standard grid setup. The magnitude of this error estimate is approximately 20%. We will use this estimate

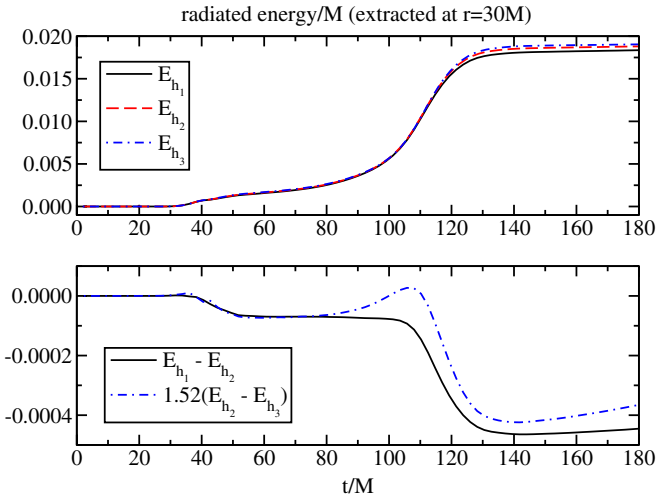

FIG. 1 (color online). This plot shows the energy radiated during the merger of a binary where both initial spins ($S/m^2 = 0.8$) are antialigned to the orbital angular momentum. The upper panel shows the energy radiated for the resolutions $h_1 = M/56.9$, $h_2 = M/61.6$, $h_3 = M/66.4$. In the lower panel we show the differences scaled for fourth order convergence.

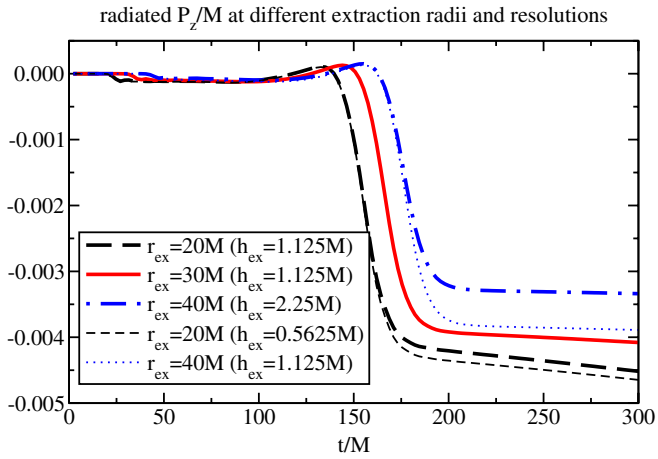

FIG. 2 (color online). The z component of the radiated momentum for the $-1, 135/-1, -135$ run. The initial spins are perpendicular to each other and lie in the initial orbital plane. This plot shows that on our relatively small grids the location of the extraction radius plays a big role and is the main contributor to the estimated approximate error of $\pm 20\%$ quoted here. The thick lines show the results with our standard grid setup. The thin lines show how these results change if we enlarge some refinement levels in order to increase the resolution $h_{\rm ex}$ at our extraction radii.

also as an approximate error bar for the kick velocities presented below, since this error is expected to be dominant.

III. RESULTS

In order to gauge possible kick sizes we have performed several simulations with different spin orientations. In each case the spin magnitude of each black hole is $S/m^2 = 0.8$ and the initial orbital angular momentum is along the z axis. The magnitude of the orbital angular momentum is chosen such that the orbits are circular according to post-Newtonian approximations [40–42]. From previous works [43–49] it follows that this approach of setting initial data puncture parameters using post-Newtonian approximations is indeed possible. The bare mass parameter m_b of each puncture is chosen such that the Arnowitt-Deser-Misner (ADM) mass m measured at each puncture is approximately $0.5M$. Because of these approximations, it is clear that the orbits will have small ellipticities. However, since we are just interested in obtaining a sample of possible kick velocities for different initial conditions, such imperfections are not critical.

We label each simulation using eight numbers: $[q, D, S_1/m^2, 90° - \theta_1, \phi_1, S_2/m^2, 90° - \theta_2, \phi_2]$. Defining the larger black hole as #2, we set $q \equiv m_2/m_1 \geq 1$. D and S_A/m^2 represent the holes' coordinate separation and the spin magnitude of hole A ($A = 1, 2$). The angles θ_A and ϕ_A (given in degrees) determine the direction of each spin by their polar angles with respect to a coordinate system $(\hat{x}, \hat{y}, \hat{z})$, where $\hat{z}$ is the unit vector in the direction of the binary's initial orbital angular momentum, $\hat{x}$ is the unit vector in the direction of the initial linear momentum of the larger hole, and $\hat{y} = \hat{z} \wedge \hat{x}$ [50]. Since our runs all have equal masses and spin magnitudes, they are all of the form $[1, 6M, 0.8, 90° - \theta_1, \phi_1, 0.8, 90° - \theta_2, \phi_2]$. The runs in Table I are thus labeled by the angles alone.

From Table I we see that almost all initial spin orientations lead to large kick velocities. The only exception is when both initial black hole spins point in exactly the same direction (see run $-31, 0/-31, 0$). In this special case no net linear momentum is radiated (in agreement with post-Newtonian predictions [41]). We find that the largest kick occurs for antialigned spins that are perpendicular to the initial angular momentum $J_\infty^{\rm ADM}$. However, we also find substantial kicks for other initial spin orientations, and in each case the kick is well above 500 km/s. This means that kicks of this magnitude should be expected for generic black hole mergers with spins of magnitude of $S/m^2 = 0.8$ or above.

This result can be explained in the following way: it is known that the black hole spins significantly influence the dynamics of the two black holes. For example, the merger can be delayed if both spins are aligned with the orbital angular momentum [51]. Or the orbits can be nonplanar as in the case of a test mass in orbit around a spinning Kerr black hole [52]. Since the linear momentum radiated depends on the orbit shape, the kick velocity also depends

TABLE I. Initial parameters and resulting kick velocities. The runs are labeled by the spin orientation angles, which for each hole are the angle between the spin and the initial orbital plane and the angle between the projection of the spin into the orbital plane and the initial linear momentum of hole 2. Here m_b is the bare mass parameter of each puncture and m the ADM mass measured at each puncture. The black holes have coordinate separation D, with puncture locations $(0, \pm D/2, 0)$ and linear momenta $(\mp P, 0, 0)$, so that the initial orbital angular momentum is in the z direction. The spins have a magnitude of $S/m^2 = 0.8$ and point in the various directions listed here, so that the total angular momentum is not necessarily along the z direction. We also list the estimates for the initial ADM mass $M_\infty^{\rm ADM}$ and ADM angular momentum $J_\infty^{\rm ADM}$. Furthermore, we give the final black hole mass M_f and angular momentum J_f, as well as the kick velocities v for the different cases.

Run	$0, 90/0, -90$	$-1, 135/-1, -135$	$45, 0/-45, 180$	$44, 180/-46, 180$	$-31, 0/-31, 0$	$-1, 180/89, 180$	$-1, 150/89, 151$	$-1, 120/89, 119$
$M_\infty^{\rm ADM}/M$	0.985	0.985	0.985	0.985	0.985	0.984	0.984	0.984
$J_\infty^{\rm ADM}/M^2$	0.842	0.882	0.839	0.881	0.756	1.016	1.016	1.016
m/M	0.50	0.50	0.50	0.50	0.50	0.50	0.50	0.50
m_b/M	0.30	0.30	0.30	0.30	0.30	0.30	0.30	0.30
D/M	6.000	6.000	6.000	6.000	6.000	6.000	6.000	6.000
P/M	0.140	0.140	0.140	0.140	0.147	0.133	0.133	0.133
L/M^2	0.842	0.840	0.839	0.839	0.881	0.798	0.798	0.798
S_{1x}/m^2	0	−0.566	0.566	−0.576	0.684	−0.800	−0.693	−0.400
S_{1y}/m^2	0.800	0.566	0	0	0	0	0.400	0.693
S_{1z}/m^2	0	−0.010	0.566	0.556	−0.414	−0.010	−0.010	−0.010
S_{2x}/m^2	0	−0.566	−0.566	−0.556	0.684	−0.010	−0.009	−0.005
S_{2y}/m^2	−0.800	−0.566	0	0	0	0	0.005	0.009
S_{2z}/m^2	0	−0.010	−0.566	−0.576	−0.414	0.800	0.800	0.800
M_f/M	0.95	0.95	0.95	0.952	0.96	0.94	0.94	0.94
J_f/M_f^2	0.67	0.72	0.68	0.73	0.64	0.81	0.80	0.80
v (km/s)	2500	1350	580	1350	0	1850	2100	1950
	±500	±250	±150	±250	±50	±350	±450	±400

strongly on spin. In fact, if the spins are not parallel to the orbital angular momentum, the spins and the orbital angular momentum both precess so that the resulting orbits do not stay in one plane and become much more complex than the familiar Newtonian circular orbits. Since the instantaneous linear momentum flux changes direction in a less regular way than for circular orbits, one expects that the averaged linear momentum flux is significantly larger than for quasicircular orbits. As an example of such a more complicated orbit, see Fig. 3 which shows the orbits of both black hole centers for the case where one of the spins starts out in the initial orbital plane and the other one perpendicular to this plane. We can clearly see that the orbits do not stay in one plane, and that the kick moves the final merged black hole downward out of the initial orbital plane.

From Figs. 1 and 2 we can see that the bulk of the radiated energy and momentum is emitted within a time of about $40M$. This is also the time during which the maximum amplitude of the gravitational waves generated by the merger passes through the detector. That is, almost the entire kick is accumulated during the final merger phase. Table I gives estimates for the mass and spin of the final black hole.

Note that for the runs listed in Table I the angle between the spins is either nearly 90° or antialigned. Judging from the aligned $-31, 0/-31, 0$ case, we expect closer alignments to have smaller kicks.

In the -1, 180/89, 180, -1, 150/89, 151, and -1, 120/89, 119 runs, the initial spin of black hole #2 is nearly perpendicular to the orbital plane, and it is almost the same in each case. The initial spin of hole #1 is approximately in the orbital plane, but the orientation differs by 30° between the -1, 180/89, 180 and -1, 150/89, 151 runs and by 60° between the -1, 180/89, 180 and -1, 120/89, 119 runs. We see that this change in orientation affects the kick velocity. This effect can be explained if we use the post-Newtonian formula (3.31b) in [41]. From this formula we see that the instantaneous rate of radiated momentum depends on the angle between the spin and the relative velocity vectors, as well as on the angle between the spin and separation vectors. Hence if we start out with different spin orientations, we expect different spin orientations also in the final merger phase where most of the final kick is accumulated, which in turn leads to different amounts of radiated momentum. A similar dependence on spin orientation is described in [34] for a system with antialigned spins in the initial orbital plane.

IV. DISCUSSION

We have performed simulations of equal mass black holes with initial spins of magnitude of $S/m^2 = 0.8$. We have tested several initial spin orientations and found that all but one lead to kick velocities well above 1000 km/s. Thus kicks between 1000 km/s and 2000 km/s seem to be a generic feature for spins of magnitude 0.8 with general orientations. Higher spins will lead to even larger kicks. This means that, for these cases, the final black hole will likely escape from dwarf elliptical and spheroidal galaxies (with escape velocities below 300 km/s), and possibly even from giant elliptical galaxies (with escape velocities around 2000 km/s) [5]. This result also has important implications for a variety of astrophysical scenarios, such as the cosmological evolution of supermassive black holes or the growth and retention of intermediate-mass black holes in dense stellar clusters. Note, however, that a more extensive parameter search should be carried out before drawing any definitive conclusions. Furthermore, notice that all our simulations are for the equal mass case. It is clear that the kick velocity will depend on the mass ratio (for two proposed models see [32,35]), and we expect smaller kicks for the unequal mass case. The probability for the large kicks obtained here might be quite low, if kick velocities drop sufficiently fast for mass ratios different from 1. In addition, it has been suggested [53] that in real galaxy mergers torques from accreting gas align the spins with the orbital angular momentum, so that the kick velocity is below 200 km/s.

Almost the entire kick is accumulated during the final merger phase, meaning that small changes in the initial conditions are likely to lead to quite different kick directions and magnitudes. The reason is that a small change in the initial velocities or separation (and also accumulated numerical errors in the orbital phase) will significantly alter the merger time [39], and thus alter the spin orientations just before merger. We therefore expect different trajectories just before the merger which then will lead to different final kicks. Note, however, that this sensitivity to initial conditions does not change our main conclusion that generic spin orientations can lead to very large kicks in the equal mass case.

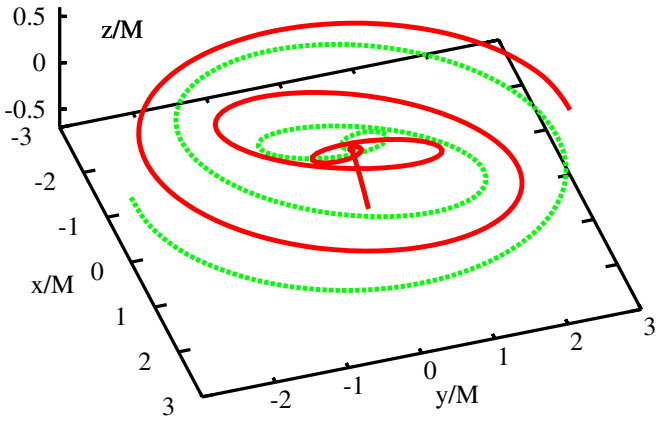

FIG. 3 (color online). This plot shows the tracks of the black hole centers for the -1, 180/89, 180 run. Here one of the initial spins is in the initial orbital plane, and the other one is perpendicular to the orbital plane. One can see that the orbits do not stay in one plane.

ACKNOWLEDGMENTS

It is a pleasure to thank B. Brügmann, J. González, M. Hannam, S. Husa, and U. Sperhake for helpful comments and code development. This work was supported by NSF Grant No. PHY-0555644. We also acknowledge partial support by the National Computational Science Alliance under Grant No. PHY060021P and No. PHY060040T. Simulations were also performed at the Charles E. Schmidt College of Science computer cluster Boca 5.

[1] TAMA, http://tamago.mtk.nao.ac.jp/.
[2] LIGO, http://www.ligo.caltech.edu/.
[3] GEO, http://geo600.aei.mpg.de/.
[4] B. Schutz, Classical Quantum Gravity **16**, A131 (1999).
[5] D. Merritt, M. Milosavljevic, M. Favata, S. A. Hughes, and D. E. Holz, Astrophys. J. **607**, L9 (2004).
[6] M. Boylan-Kolchin, C.-P. Ma, and E. Quataert, Astrophys. J. **613**, L37 (2004).
[7] Z. Haiman, Astrophys. J. **613**, 36 (2004).
[8] P. Madau and E. Quataert, Astrophys. J. **606**, L17 (2004).
[9] J. Yoo and J. Miralda-Escude, Astrophys. J. **614**, L25 (2004).
[10] M. Volonteri and R. Perna, Mon. Not. R. Astron. Soc. **358**, 913 (2005).
[11] N. I. Libeskind, S. Cole, C. S. Frenk, and J. C. Helly, Mon. Not. R. Astron. Soc. **368**, 1381 (2006).
[12] M. Micic, T. Abel, and S. Sigurdsson, arXiv:astro-ph/0512123.
[13] M. C. Miller and D. P. Hamilton, Mon. Not. R. Astron. Soc. **330**, 232 (2002).
[14] M. C. Miller and D. P. Hamilton, Astrophys. J. **576**, 894 (2002).
[15] H. Mouri and Y. Taniguchi, Astrophys. J. **566**, L17 (2002).
[16] H. Mouri and Y. Taniguchi, Astrophys. J. **580**, 844 (2002).
[17] K. Gultekin, M. C. Miller, and D. P. Hamilton, Astrophys. J. **616**, 221 (2004).
[18] K. Gultekin, M. Coleman Miller, and D. P. Hamilton, Astrophys. J. **640**, 156 (2006).
[19] R. M. O'Leary, F. A. Rasio, J. M. Fregeau, N. Ivanova, and R. O'Shaughnessy, Astrophys. J. **637**, 937 (2006).
[20] A. G. Wiseman, Phys. Rev. D **46**, 1517 (1992).
[21] M. Favata, S. A. Hughes, and D. E. Holz, Astrophys. J. **607**, L5 (2004).
[22] L. Blanchet, M. S. S. Qusailah, and C. M. Will, Astrophys. J. **635**, 508 (2005).
[23] T. Damour and A. Gopakumar, Phys. Rev. D **73**, 124006 (2006).
[24] C. F. Sopuerta, N. Yunes, and P. Laguna, Phys. Rev. D **74**, 124010 (2006).
[25] C. F. Sopuerta, N. Yunes, and P. Laguna, Astrophys. J. **656**, L9 (2007).
[26] J. D. Schnittman and A. Buonanno, arXiv:astro-ph/0702641.
[27] F. Herrmann, D. Shoemaker, and P. Laguna, arXiv:gr-qc/0601026.
[28] J. G. Baker *et al.*, Astrophys. J. **653**, L93 (2006).
[29] J. A. Gonzalez, U. Sperhake, B. Bruegmann, M. Hannam, and S. Husa, Phys. Rev. Lett. **98**, 091101 (2007).
[30] F. Herrmann, I. Hinder, D. Shoemaker, P. Laguna, and R. A. Matzner, arXiv:gr-qc/0701143.
[31] M. Koppitz *et al.*, arXiv:gr-qc/0701163 [Phys. Rev. Lett. (to be published)].
[32] M. Campanelli, C. O. Lousto, Y. Zlochower, and D. Merritt, Astrophys. J. **659**, L5 (2007).
[33] J. A. Gonzalez, M. D. Hannam, U. Sperhake, B. Brugmann, and S. Husa, Phys. Rev. Lett. **98**, 231101 (2007).
[34] M. Campanelli, C. O. Lousto, Y. Zlochower, and D. Merritt, Phys. Rev. Lett. **98**, 231102 (2007).
[35] J. G. Baker *et al.*, arXiv:astro-ph/0702390.
[36] M. Campanelli, C. O. Lousto, P. Marronetti, and Y. Zlochower, Phys. Rev. Lett. **96**, 111101 (2006).
[37] J. G. Baker, J. Centrella, D.-I. Choi, M. Koppitz, and J. van Meter, Phys. Rev. Lett. **96**, 111102 (2006).
[38] B. Bruegmann, W. Tichy, and N. Jansen, Phys. Rev. Lett. **92**, 211101 (2004).
[39] B. Bruegmann, J. Gonzalez, M. Hannam, S. Husa, U. Sperhake, and W. Tichy, arXiv:gr-qc/0610128.
[40] P. Marronetti, W. Tichy, B. Bruegmann, J. Gonzalez, M. Hannam, S. Husa, and U. Sperhake, Classical Quantum Gravity **24**, S43 (2007).
[41] L. E. Kidder, Phys. Rev. D **52**, 821 (1995).
[42] W. Tichy, E. E. Flanagan, and E. Poisson, Phys. Rev. D **61**, 104015 (2000).
[43] W. Tichy, B. Brügmann, M. Campanelli, and P. Diener, Phys. Rev. D **67**, 064008 (2003).
[44] W. Tichy and B. Brügmann, Phys. Rev. D **69**, 024006 (2004).
[45] W. Tichy, B. Brügmann, and P. Laguna, Phys. Rev. D **68**, 064008 (2003).
[46] M. Ansorg, B. Brügmann, and W. Tichy, Phys. Rev. D **70**, 064011 (2004).
[47] N. Yunes, W. Tichy, B. J. Owen, and B. Bruegmann, arXiv:gr-qc/0503011.
[48] N. Yunes and W. Tichy, Phys. Rev. D **74**, 064013 (2006).
[49] B. J. Kelly, W. Tichy, M. Campanelli, and B. F. Whiting, Phys. Rev. D **76**, 024008 (2007).
[50] In this paper, we constructed our initial data sets such that the numerical grid coordinate system (x, y, z) coincides with $(\hat{x}, \hat{y}, \hat{z})$.
[51] M. Campanelli, C. O. Lousto, and Y. Zlochower, Phys. Rev. D **74**, 041501 (2006).
[52] M. Campanelli, C. O. Lousto, Y. Zlochower, B. Krishnan, and D. Merritt, Phys. Rev. D **75**, 064030 (2007).
[53] T. Bogdanovic, C. S. Reynolds, and M. C. Miller, arXiv:astro-ph/0703054.